Evidence for a Regulatory Role of Cholesterol Superlattices in the Hydrolytic Activity of Secretory Phospholipase A2 in Lipid Membranes[†]

Fang Liu and Parkson Lee-Gau Chong*

Department of Biochemistry, Temple University School of Medicine, Philadelphia, Pennsylvania 19140

Received November 11, 1998; Revised Manuscript Received January 19, 1999

ABSTRACT: We have conducted a detailed study of the effect of membrane cholesterol content on the initial hydrolytic activity of *Crotalus durissus terrificus* venom phospholipase A2 (sPLA2) in large unilamellar vesicles of cholesterol/dimyristoyl-L-α-phosphatidylcholine (DMPC) and cholesterol/1-palmitoyl-2-oleoyl-L-α-phosphatidylcholine (POPC) at 37 °C. The activity was monitored by using the acrylodan-labeled intestinal fatty acid binding protein and HPLC. In contrast to conventional approaches, we have used small cholesterol concentration increments (∼0.3−1.0 mol %) over a wide concentration range (e.g., 13−54 mol % cholesterol). In both membrane systems examined, the initial hydrolytic activity of sPLA2 is found to change with cholesterol content in an alternating manner. The activity reaches a local minimum when the membrane cholesterol content is at or near the critical cholesterol mole fractions (e.g., 14.3, 15.4, 20.0, 22.2, 25.0, 33.3, 40.0, and 50.0 mol % cholesterol) predicted for cholesterol regularly distributed in either hexagonal or centered rectangular superlattices. According to the sterol regular distribution model [Chong, P. L.-G. (1994) *Proc. Natl. Acad. Sci. U.S.A. 91*, 10069−10073; Liu et al. (1997) *Biophys. J. 72*, 2243−2254], the extent of lipid superlattices is maximal at the critical cholesterol mole fractions, at which the membrane free volume is minimal. Thus, our present data can be taken to indicate that the initial hydrolytic activity of sPLA2 is governed by the extent of cholesterol superlattice. These data provide the first functional evidence for the formation of cholesterol superlattices in both saturated (e.g., DMPC) and unsaturated (e.g., POPC) liquid-crystalline phospholipid bilayers. The data also illustrate the functional importance of cholesterol superlattice and demonstrate a new type of regulation of sPLA2. Furthermore, upon binding to cholesterol/POPC large unilamellar vesicles, the intrinsic fluorescence intensity of sPLA2 shows an alternating variation with cholesterol content, exhibiting a minimum at the critical cholesterol mole fractions. This result suggests that either the number of sPLA2 bound to lipid vesicles or the conformation of membrane-bound sPLA2 or both vary with the extent of the cholesterol superlattice in the plane of the membrane.

Secretory phospholipase A_2 (sPLA2; EC 3.1.1.4.; ∼13−15 kDa) is a group of extracellular water-soluble enzymes which catalyze the hydrolysis of the *sn*-2 fatty acid ester of phospholipids to lysophospholipids and free fatty acids. The activity of sPLA2 is Ca^{2+}-dependent. The amino acid sequences and secondary and X-ray crystal structures of many sPLA2s have been determined (reviewed in ref *1*). sPLA2 acts favorably with the aggregated form of phospholipid substrates, rather than the monomeric phospholipids (*2*−*4*). One current paradigm for how sPLA2 works is (reviewed in ref *5*) that sPLA2 in the aqueous phase (E) first binds to the surface of the phospholipid bilayer (S) to form an activated enzyme (E*). E* then binds a monomeric phospholipid molecule in the catalytic site to form an E*S complex (*6*). The catalytic site of sPLA2 is ∼14 Å away from the bilayer surface (*7*). E*S is subsequently converted to E*P, which is the enzyme bound to the bilayer with the hydrolyzed lipid products (i.e., free fatty acids and lysophospholipids) in the catalytic site. The enzyme E*P then proceeds to release the products.

sPLA2 acts favorably with phospholipid bilayers which contain membrane defects (*8*, *9*, and references therein). For example, bee venom sPLA2 binding is enhanced by membrane defects induced by *n*-alcohols (*10*). Ceramide induces defects in dipalmitoyl-L-α-phosphatidylcholine (DPPC) bilayers and consequently activates cobra venom sPLA2 (*11*). Structural irregularities in the gel state of lipid bilayers activate the binding of porcine pancreatic sPLA2 to lipid vesicles (*12*−*14*). Lateral phase separation of phospholipid substrates and reaction products in the membrane modulates pancreatic sPLA2 (*15*). There exists also a strong correlation between lipid lateral microheterogeneity and the burst phase of sPLA2 activity (*9*). Note that both structural irregularities and the interfacial boundaries between separated lipid phases (microheterogeneity) are able to create membrane defects. Thus, all of these studies suggested that membrane defects

[†] This work was supported by grants from the American Heart Association (951073 and S98761S).

* To whom correspondence should be addressed. Phone: 215-707-4182. Fax: 215-707-7536. E-mail: plchong@vm.temple.edu.

[1] Abbreviations: ADIFAB, 6-acryloyl-2-dimethylaminonaphthalene (acrylodan)-labeled intestinal fatty acid binding protein; DMPC, dimyristoyl-L-α-phosphatidylcholine; DPPC, dipalmitoyl-L-α-phosphatidylcholine; DOPC, dioleoyl-L-α-phosphatidylcholine; POPC, 1-palmitoyl-2-oleoyl-L-α-phosphatidylcholine; LUV, large unilamellar vesicles; MLV, multilamellar vesicles; Pyr-PC, 1-palmitoyl-2-(10-pyrenyl)-decanoyl-*sn*-glycerol-3-phosphatidylcholine; sPLA2, secretory phospholipase A_2.

10.1021/bi982693q CCC: $18.00
Published on Web 03/11/1999

play an important role in the catalytic activity and membrane binding of sPLA2.

Membrane defects (or membrane free volume) have recently been shown to vary with cholesterol content in an alternating manner in phospholipid bilayers (*16*−*18*). Specifically, membrane defects exhibit a local minimum at the critical cholesterol mole fractions (e.g., 14.3, 15.4, 20.0, 22.2, 25.0, 33.3, 40.0, and 50.0 mol %), at which cholesterol molecules are predicted to be regularly distributed into either hexagonal (*19*) or centered rectangular (*20*) superlattices. According to the sterol regular distribution model (*19*), regularly and irregularly distributed lipid areas coexist in a given sterol-containing membrane, but the ratio of these two distributions reaches a local maximum at the critical sterol mole fractions (*21*). On the basis of these new findings and concepts, we have previously hypothesized (*16*, *18*, *19*, *22*) that membrane properties, especially those being influenced by membrane defects (or membrane free volume), are modulated by sterol content in an alternating manner. This hypothesis has recently proven to be correct in the partitioning of an antifungal drug, nystatin, into lipid membrane (*23*).

In the present study, we have tested the above hypothesis on the hydrolytic activity of sPLA2. A role for the membrane cholesterol content in the activity of sPLA2 would be expected because the binding of sPLA2 to lipid bilayers is influenced by membrane defects, which are known to vary with cholesterol content due to changes in the extent of cholesterol superlattice, as mentioned earlier. To test this hypothesis, we have examined the membrane cholesterol concentration dependence of the initial hydrolytic activity of *Crotalus durissus terrificus* venom sPLA2 at 37 °C in large unilamellar vesicles composed of cholesterol/dimyristoyl-L-α-phosphatidylcholine (DMPC) or cholesterol/1-palmitoyl-2-oleoyl-L-α-phosphatidylcholine (POPC). Both ADIFAB (6-acryloyl-2-dimethylaminonaphthalene (acrylodan)-labeled intestinal fatty acid binding protein) and HPLC (high-performance liquid chromatography) have been used to monitor the hydrolytic activity of sPLA2. In contrast to conventional approaches, we have used small (∼0.3−1.0 mol %) cholesterol concentration increments over a wide concentration range (e.g., 13−54 mol % cholesterol). In both membrane systems examined, the initial hydrolytic activity of sPLA2 is found to change with cholesterol content in a well-defined alternating manner in accordance with the sterol regular distribution model (*18*−*20*).

MATERIALS AND METHODS

Materials. Cholesterol (Sigma, St. Louis) was recrystallized from ethanol. The concentration of cholesterol stock solution (in chloroform) was calculated from weight determinations. DMPC and POPC were purchased from Avanti Polar Lipids (Alabaster, AL) and used as such. The concentrations of phospholipid stock solutions (in chloroform) were determined by the method of Bartlett (*24*). Fatty acid standards such as myristic acid and oleic acid were obtained from Sigma. The acrylodan-labeled recombinant rat intestinal fatty acid binding protein (ADIFAB) was purchased from Molecular Probes (Eugene, OR), and its concentration was determined using an extinction coefficient at 365 nm equal to 10600 M^{-1} cm^{-1} (in 0.1 M Tris buffer, pH 7.4) (*25*). *Crotalus durissus terrificus* venom phospholipase A_2 (sPLA2) was obtained from Sigma. The concentration of sPLA2 was determined by the Lowry method (*26*) using bovine serum albumin as the standard.

Vesicle Preparation. Appropriate amounts of cholesterol and phospholipids were first mixed in chloroform. The mixture was then dried under nitrogen in microtubes (Perfector Scientific, Atascadero, CA) and placed under high vacuum overnight. The dried mixtures were suspended in 0.1 M Tris buffer (pH 7.4) containing 0.02% NaN_3. The dispersion was vortexed for 3 min at temperatures (43 °C for DMPC and 24 °C for POPC) well above the main phase transition temperatures of the matrix phospholipids. The resulting multilamellar vesicles were cooled to 4 °C for 30 min and then incubated at 43 °C for 30 min for vesicles containing DMPC, or cooled to −20 °C for 30 min and then incubated at 24 °C for 30 min for vesicles containing POPC. This cooling/heating cycle was repeated two more times. Finally the samples were stored under nitrogen at room temperature (∼24 °C) for ∼7 days prior to extrusion. The cooling/heating cycles and long incubation provide a means of evenly distributing membrane components among lipid multilayers and attaining an equilibrium distribution of molecules within each monolayer (discussed in ref *18*). To form large unilamellar vesicles (LUV), we extruded multilamellar vesicles 10 times using a lipid extruder (Lipex, Vancouver, Canada) (*27*) through two stacked 0.8 μm polycarbonate membranes at the same temperatures as those used for vortexing. LUVs were incubated at room temperature for ∼4 days prior to activity or binding measurements. After extrusion, the cholesterol/phospholipid molar ratios in vesicles (LUVs) remained virtually unchanged, as determined by the Bartlett method (*24*) and the cholesterol oxidase assay (*28*) (Wang and Chong, unpublished results). For all of the activity and binding measurements (see below), the temperature of the sample was kept at 37 ± 0.2 °C by a circulating bath. At this temperature, all of the bilayer membranes examined were in the liquid-crystalline state.

s*PLA2 Activity Measurements*. The initial hydrolytic activity of sPLA2 was measured by two different methods. In the first method, a water-soluble acrylodated intestinal fatty acid binding protein (ADIFAB) was used as a free fatty acid fluorescence indicator (*25*). Free fatty acids released from lipid vesicles by sPLA2 hydrolysis are taken up by ADIFAB; this gives rise to a shift in the emission maximum of ADIFAB fluorescence from 432 to 505 nm (*29*). The resulting decrease in the peak height at 432 nm is proportional to the amount of fatty acid hydrolyzed by sPLA2 (*29*, *30*). Specifically, a reaction solution was prepared by adding 50 μL of 0.34 M $CaCl_2$ and 5 μL of ADIFAB (500 units/mL in 0.1 M Tris buffer, pH 7.4) into a fluorescence cuvette containing 1.65 mL of LUVs in 0.02% NaN_3 and 0.1 M Tris buffer (pH 7.4). The mixture was incubated at 37 °C for 15 min. To initiate the hydrolysis reaction, we injected 10 μL of sPLA2 (0.8 mg/mL in 0.1 M Tris buffer, pH 7.4, and 10 mM $CaCl_2$) into the reaction solution. The final phospholipid and Ca^{2+} concentrations in the cuvette were 6.2 μM and 10 mM, respectively. Immediately after the injection, the intensity of ADIFAB fluorescence at 432 nm was recorded over time using an 8-nm band-pass in the emission monochromator. The fluorescence intensity changes virtually linearly with time in the first minute (data not shown). The slope of the fluorescence intensity change in the first minute

upon addition of sPLA2 was taken as the initial hydrolytic rate of phospholipids by sPLA2. This apparent initial hydrolytic activity, in terms of fluorescence intensity change at 432 nm/s, was then converted to the amount of fatty acid hydrolyzed per second using a standard curve. The standard curve was constructed by measuring the changes of ADIFAB fluorescence intensity at 432 nm in the presence of varying amounts of standard fatty acids, namely, myristic acid (for cholesterol/DMPC bilayer substrate) or oleic acid (for cholesterol/POPC bilayers). All of the ADIFAB fluorescence measurements were made, while stirring, on a SLM 8000C fluorometer (Urbana, IL) using excitation at 378 nm with a 2 nm band-pass in the excitation monochromator. Blank readings from vesicles in the absence of ADIFAB were negligible.

Note that, in this measurement, as well as in other activity and binding measurements throughout this work, we have focused on the events that take place in the first minute because only the initial events can be linked meaningfully to cholesterol regular distribution. After the hydrolytic reaction proceeds for a prolonged time, the exact lipid composition in the bilayer membrane is not known. Membrane lipid composition is important in the present study because it determines the extent of lipid superlattice (*16*, *18*, *19*, *23*, *31*−*34*). It should also be mentioned that no latency phase (ref *35* and references therein) was observed in the time period examined (up to 4 h, data not shown). This observation is consistent with a previous finding (*29*) that *Crotalus durissus terrificus* sPLA2 does not display a latency phase in cholesterol/dioleoyl-L-α-phosphatidylcholine (DOPC) LUVs (cholesterol/DOPC = $^1/_2$) at 37 °C (up to 20 min). Serum albumin was not used in this study in order to exclude inhibition (*36*) or stimulation (*37*, *38*) of the sPLA2 activity by the reaction products. This is because albumin might interfere with the ADIFAB assay due to the buffering capacity of albumin for fatty acids (*29*).

The activity of sPLA2 was also measured by HPLC. First, a solution of 1.7 mL of LUV dispersion containing 58.8 μM phospholipid, 10 mM $CaCl_2$, 0.02% NaN_3, and 0.1 M Tris buffer (pH 7.4) was incubated with stirring in a screw-capped tube at 37 °C for 15 min. To this reaction mixture was added 100 μL of 0.8 mg/mL sPLA2 (in the same buffer) to initiate the hydrolysis reaction. After the reaction proceeded for 1 min, the reaction was stopped by the addition of 200 μL of saturated EGTA (in deionized water). The reaction mixture was then mixed with 20 μL of 0.467 mM standard palmitic acid in methanol, followed by the addition of 8 mL of chloroform to extract both the fatty acids hydrolyzed by sPLA2 and the internal standard palmitic acid. The bottom organic layer was collected and dried under nitrogen. To make the fatty acids more readily detectable by absorption, we esterified the free fatty acids. Specifically, the free fatty acids were reacted with 25 μL of 10 mg/mL 2-bromo-2′-acetonaphthone (in acetone) and 25 μL of 10 mg/mL triethylamine (in acetone) in a boiling water bath for 15 min (*39*). Then, 35 μL of 2 mg/mL acetic acid in acetone was added to the reaction mixture and heated at 100 °C for an additional 5 min. The reaction mixture was evaporated to dryness with nitrogen and then redissolved in 200 μL of acetonitrile. A 30 μL aliquot of the solution was subsequently injected into a HPLC column (Waters, reversed-phase C18 μBondapak, 250 × 4.6 mm) and eluted with 87% acetonitrile and 13% water using a flow rate of 2 mL/min (Beckman, model 324). The eluted products were detected by absorbance at 254 nm. In the present study, the HPLC method was employed only for the sPLA2 activity measurements with cholesterol/DMPC bilayers as the substrate. The first absorbance peak appeared at a retention time of ∼16 min. This peak corresponded to the myristic acid resulting from sPLA2-induced hydrolysis of DMPC, as verified by a separated HPLC run using an external myristic acid standard. The second major peak appeared at a retention time of ∼32 min, which corresponded to the internal standard palmitic acid. The amount of myristic acid (μg) hydrolyzed by sPLA2 (Y) was calculated from the peak heights (H) by the equation $Y = (H_{16}/H_{32})$(micrograms of standard palmitic acid injected into HPLC)(M_m/M_p). H_{16} and H_{32} are the peak heights at the 16 and 32 min retention times, respectively, and M_m and M_p are the molecular weights of myristic and palmitic acids, respectively.

Binding of sPLA2 to Bilayer Substrate. The binding study was performed using a solution containing 32 μg of sPLA2, 10 mM $CaCl_2$, and 0.1 M Tris buffer (pH 7.4). To this solution, preincubated at 37 °C for 15 min, was added an aliquot of cholesterol/POPC LUVs. After sPLA2 was mixed with lipid vesicles at 37 °C for 1 min, the emission spectrum of sPLA2 intrinsic fluorescence (band-pass = 8 nm) was recorded, while stirring, using excitation at 280 nm (band-pass = 2 nm). Background readings without sPLA2 were subtracted from sample readings. The decrease of the intrinsic fluorescence intensity of sPLA2 at 340 nm upon binding to lipid vesicles is designated as ΔF ($= F_o - F$), where F and F_o are the fluorescence intensities of sPLA2 at 340 nm with and without bilayer substrate, respectively. F was corrected for volume changes. $\Delta F/F_o$ represents the percent decrease of sPLA2 fluorescence intensity upon binding to lipid bilayers as a result of changes in quantum yield; thus, $\Delta F/F_o$ is a measure of the extent of sPLA2 binding.

RESULTS AND DISCUSSION

The results with regard to the effect of membrane cholesterol content on the initial hydrolytic activity of sPLA2 in cholesterol/DMPC LUVs, as monitored by the ADIFAB assay, are presented in Figure 1A. As shown in Figure 1A, there is a general decrease in hydrolytic activity when the membrane cholesterol content is increased from 13 to 54 mol %. This general trend can be attributed to the cholesterol condensing effect on liquid-crystalline phospholipid acyl chains (*40*, *41*) and to the decreased substrate availability (i.e., the decrease in the percent of DMPC). This general trend has previously been observed by others (e.g., ref *42*) in studies using large cholesterol concentration increments (e.g., 10 mol %).

In contrast to previous studies, we have used here small cholesterol concentration increments (∼0.3−1.0 mol %) and found that the sPLA2 activity does not change monotonically with cholesterol. Instead, the activity exhibits dips at 14.3, 15.6, 20.0, 22.6, 24.3, 28.0, 33.3, 40.5, 46.0, and 49.5 mol % cholesterol (indicated by arrows at bottom of Figure 1A). These dip positions, except for 28.0 and 46.0 mol %, are at or close to the critical cholesterol mole fractions (i.e., 14.3, 15.4, 20.0, 22.2, 25.0, 33.3, 40.0, and 50.0 mol %) predicted for cholesterol being regularly distributed into hexagonal or

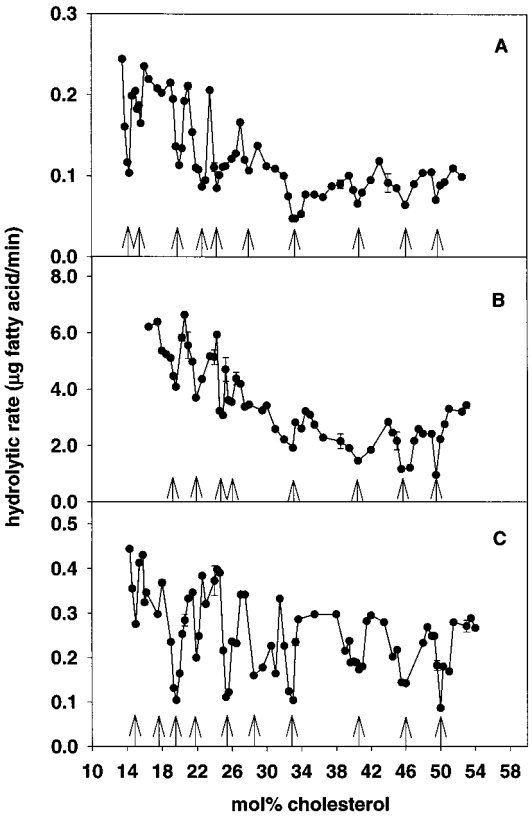

FIGURE 1: Effects of membrane cholesterol content on the initial rate of sPLA2-catalyzed hydrolysis of (A) DMPC in cholesterol/DMPC LUVs as monitored by the ADIFAB assay, (B) DMPC in cholesterol/DMPC LUVs as monitored by the HPLC method, and (C) POPC in cholesterol/POPC LUVs as monitored by the ADIFAB assay. Temperature = 37 °C. Vesicle pore size = ~800 nm. The molar ratio of sPLA2 to PC was ~1/18:1/19. The arrows at the bottom indicate the positions of the hydrolytic activity minimum. The vertical bars represent the standard deviations obtained from three independently prepared samples. The arrows and vertical bars in Figure 2B bear the same meaning.

centered rectangular superlattices (*18*−*20*, *23*). A plot of the theoretically predicted critical cholesterol mole fractions versus the activity dip positions (excluding 28.0 and 46.0 mol % dips) gives an excellent correlation coefficient, *r*, of 0.9995. These data provide compelling functional evidence that cholesterol can be regularly distributed into superlattices in liquid-crystalline DMPC bilayers. Note that several lines of strong and consistent semifunctional (*23*) and spectroscopic (*16*, *18*−*20*, *43*) evidence for sterol regular distribution in liquid-crystalline bilayers have previously been reported.

The activity dips at 28.0 and 46.0 mol % are not those theoretically predicted; their appearance may result from the coexistence of two or more types of superlattices (*21*, *32*). These putative complex lateral organizations may arise from compositional heterogeneity in lipid vesicles. It is likely that, in certain sample preparations, not all of the vesicles contain the same amounts of cholesterol. It is also likely that there exists some heterogeneity between superlattices in the inner and outer monolayers.

While the ADIFAB assay provides the most sensitive and a continuous measurement of sPLA2 activity (*29*), this assay measures the free fatty acid concentration in the aqueous phase, which depends on the membrane/water partition coefficient of fatty acid. To demonstrate that the alternating pattern shown in Figure 1A is due to cholesterol-induced changes in enzyme activity, rather than cholesterol-induced changes in fatty acid partition coefficient, we have also determined the cholesterol concentration dependence of the initial activity of sPLA2 by the HPLC method. This method determines the total fatty acid hydrolyzed by sPLA2. As shown in Figure 1B, the initial hydrolytic activity of sPLA2 determined by the HPLC method also exhibits an alternating variation with cholesterol content. In this case, the activity dips appear at 19.6, 21.9, 25.0, 26.0, 33.0, 40.5, 45.5, and 49.5 mol % cholesterol in DMPC LUVs at 37 °C. Within the experimental errors (~10% in the activity measurements and ~0.5 mol % in the cholesterol concentration determinations (*18*)), these dip positions, except for 26.0 and 45.5 mol % (discussed before), agree with ($r = 0.9995$) the theoretically predicted critical cholesterol mole fractions (20.0, 22.2, 25.0, 33.3, 40.0, and 50.0 mol %) (*18*−*20*, *23*). This result is consistent with that obtained from the ADIFAB experiment (Figure 1A). Together, our data (Figure 1A,B) show that the initial hydrolytic activity of sPLA2 in liquid-crystalline cholesterol/DMPC LUVs can be modulated in an alternating manner by membrane cholesterol content. The activity is minimal at cholesterol concentrations at which the extent of cholesterol superlattice in the plane of the membrane is maximal (*18*, *19*, *21*, *23*).

Figure 1C shows that the alternating variation of sPLA2 activity (monitored by the ADIFAB assay) with cholesterol content also occurs in cholesterol/POPC LUVs at 37 °C. In this case, the authentic activity dips appear at 15.0, 17.5, 19.6, 21.9, 25.3, 28.5, 33.0, 40.3, 46.0, and 50.0 mol % cholesterol. Within the experimental errors, all of these mole fractions, except for 17.5, 28.5, and 46.0 mol %, are consistent with ($r = 0.9998$) the critical cholesterol mole fractions (e.g., 15.4, 20.0, 22.2, 25.0, 33.3, 40.0, and 50.0 mol %) predicted for maximal superlattice formation. The possible physical origin of the unexpected activity dips has been discussed earlier. For the purpose of exploring the regulatory role of cholesterol superlattice, it is immaterial how two or three unexpected activity dips actually occur. What is important is the finding that an activity dip is always observed at or near the theoretically predicted critical cholesterol mole fractions (Figure 1).

The biphasic variation of sPLA2 activity in the vicinity of critical cholesterol mole fractions (Figure 1) can be understood by virtue of the sterol regular distribution model (*19*). The model states that the membrane free volume varies with sterol content in an alternating manner, with the smallest membrane free volume present at critical sterol mole fractions where the extent of superlattices is maximal (*16*−*19*, *23*). The binding and the hydrolytic activity of sPLA2 depend on membrane defects (or membrane free volume), as mentioned earlier. Thus, the observation that sPLA2 activity is minimal at critical sterol mole fractions (Figure 1) can be understood in terms of changes in membrane defects (or membrane free volume) via changes in the extent of lipid superlattices. It is important to mention that, at present, there is no alternative explanation for the observed results. Our data cannot be attributed to the formation of crystals of cholesterol monohydrate because recent X-ray diffraction studies showed that cholesterol crystals do not occur in POPC until 67 mol % cholesterol (*44*), which is beyond the concentration range examined in our present study. Our data cannot be interpreted as the result of the formation of

cholesterol-rich microdomains either. First, there are no theoretical grounds for why cholesterol-rich microdomains should occur at the critical cholesterol mole fractions (e.g., 14.3, 15.4, 20.0, 22.2, 25.0, 33.3, 40.0, and 50.0 mol % cholesterol). Second, if sterol-rich microdomains formed at the critical sterol mole fractions, we should have observed a decrease in steady-state anisotropy of dehydroergosterol fluorescence at the critical mole fractions due to self-energy transfer. On the contrary, our previous work (*18*) showed an increase in dehydroergosterol anisotropy at the critical sterol mole fractions. Our data cannot be interpreted as the result of the vesicle type either because similar sPLA2 activity dips were observed near the critical mole fractions in cholesterol/DMPC multilamellar vesicles (MLVs) (data not shown). Further, MLVs are known to have a much more heterogeneous size distribution than LUVs; yet, we can detect sPLA2 activity dips at critical mole fractions in both types of vesicles. This indicates that the homogeneity of the vesicle size is not essential for the alternating variation of sPLA2 activity with cholesterol content.

Recall that a similar biphasic variation of the initial hydrolytic activity of *Crotalus durissus terrificus* venom sPLA2 with the mole fraction of a bulky lipid, namely, 1-palmitoyl-2-(10-pyrenyl)decanoyl-*sn*-glycerol-3-phosphatidylcholine (Pyr-PC), has previously been observed at 66.7 mol % Pyr-PC in DMPC LUVs (diameter ~400 nm) at 37 °C (*16*). The value 66.7 mol % is one of the critical Pyr-PC mole fractions at which lipids are regularly distributed into hexagonal superlattices in Pyr-PC/DMPC mixtures (*22*, *32*). From Figure 1 and the previous data obtained from Pyr-PC/DMPC bilayers (*16*), it can be concluded that the hydrolytic activity of sPLA2 is modulated by the fractional concentration of bulky lipids according to the physical principles of lipid superlattice formation (*22*, *45*). Using the same rationale, the hydrolytic activity of sPLA2 would be predicted to also vary with phosphatidylethanolamine (PE) content in an alternating manner in PE/phosphatidylcholine (PC) mixtures, because evidence for the formation of the headgroup superlattice has recently been reported in the PE/PC mixture (*33*).

To test whether the alternating variation of sPLA2 activity with cholesterol results from changes in sPLA2 binding to membranes, we have examined the effect of membrane cholesterol content on the intrinsic fluorescence intensity of sPLA2. The intrinsic fluorescence intensity of sPLA2 decreases when it is bound to lipid bilayers, as illustrated in Figure 2A; therefore, the magnitude of the intensity decrease reflects the extent of sPLA2 binding to bilayers. The striking result is that the decrease of the sPLA2 fluorescence intensity is significantly less when bound to vesicles at the critical cholesterol mole fractions (e.g., 22.2 mol % in Figure 2A (○)), as compared to that at the noncritical cholesterol mole fractions (e.g., 21.5 (▽) and 23.0 mol % (●) in Figure 2A). Figure 2B displays the cholesterol concentration dependence of the percent decrease of sPLA2 fluorescence intensity at 340 nm ($\Delta F/F_o$, defined in Materials and Methods) upon binding to cholesterol/POPC LUVs for 1 min at 37 °C. $\Delta F/F_o$ varies with cholesterol in an alternating manner in the concentration range of 18−26 mol %, showing local minimums at 19.6, 22.2, and 25.0 mol % cholesterol (Figure 2B). These mole fractions are at or very close to the critical cholesterol mole fractions (i.e., 20.0, 22.2, and 25.0 mol %)

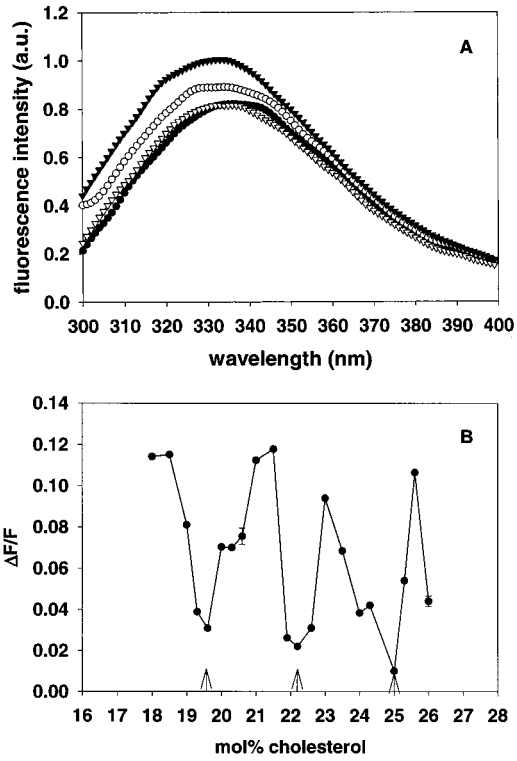

FIGURE 2: (A) Corrected emission spectra of sPLA2 intrinsic fluorescence in buffer alone (▼) and in the presence of cholesterol/POPC LUVs at 37 °C (▽, 21.5 mol % cholesterol; ○, 22.2 mol %; and ●, 23.0 mol %). (B) Effect of membrane cholesterol content on the percent decrease of sPLA2 intrinsic fluorescence intensity ($\Delta F/F_o$) upon binding to cholesterol/POPC LUVs (pore size ~800 nm) at 37 °C. The molar ratio of sPLA2 to POPC was ~1/50. Fluorescence was recorded immediately after sPLA2 and vesicles were mixed and incubated at 37 °C for 1 min.

predicted for maximal superlattice formation (*18*, *19*, *23*). These data suggest that the number of sPLA2 bound to cholesterol/POPC LUVs may be reduced to a local minimum at the critical cholesterol mole fractions. Conceivably, the fewer sPLA2 molecules bind to lipid bilayers, the less the sPLA2 hydrolytic activity is. Furthermore, at the critical cholesterol mole fractions, membrane defects have been shown to exhibit a local minimum (*17*, *18*). Thus, taken together, our studies support the previous finding that sPLA2 binding is in favor of membrane defects (*8*, *9*, and references therein).

Alternatively, it is possible that the conformation of sPLA2 varies with the extent of cholesterol superlattice. sPLA2 may have less conformational change upon binding to bilayers at the critical cholesterol mole fractions than at the noncritical cholesterol mole fractions, as a result of membrane free volume variations. This explanation is supported by the emission spectra of sPLA2 fluorescence (Figure 2A). In the absence of vesicles (▼ in Figure 2A), the emission maximum appears at 333 nm. Once bound to vesicles at the critical cholesterol mole fractions (e.g., 22.2 mol % cholesterol in POPC LUVs; ○ in Figure 2A), sPLA2 exhibits an emission maximum at 334 nm. When bound to vesicles at the noncritical cholesterol mole fractions (e.g., 21.5 (▽) and 23.0 (●) mol % in Figure 2A), the emission maximum undergoes a further red shift to 336 nm. A difference in the emission maximum of protein intrinsic fluorescence is usually indicative of protein conformational change. However, further studies using more sophisticated techniques are required to

quantitatively evaluate the cholesterol concentration dependence of sPLA2 conformation. At present, it can be tentatively concluded that either the number of sPLA2 bound to lipid vesicles or the conformation of membrane-bound sPLA2 or both vary with the extent of cholesterol superlattice in the plane of the membrane.

In any case, the present results have some important biophysical implications. First, the sPLA2 used in this study contains mainly component B of crotoxin from the South American rattlesnake *Crotalus durissus terrificus*. Component B is a single polypeptide chain with its amino acid sequence similar to those of PLA2 from mammalian pancreas and snake venom (*47*, *48*). Regardless of the binding mechanism (*49*), many of these PLA2s have been demonstrated to act favorably when membrane defects in bilayer substrate are abundant (ref *9* and references therein). Therefore, the physical principles revealed in this study are likely to be applicable to many other PLA2s such as 85 kDa cytosolic phospholipase A2, which plays a pivotal role in the biosynthesis of the eicosanoids. Second, lipid vesicles are widely used as the substrates of membrane surface acting enzymes such as sPLA2 and protein kinase C. The present results point out that, when using cholesterol-containing lipid bilayers as the substrate of sPLA2 (or other surface acting enzymes), there is a need to use vesicles that have been thoroughly mixed and subject to a long incubation, as described in this paper. The relationship between enzyme activities and cholesterol lateral organization can be assessed meaningfully only when the lateral distribution of cholesterol reaches a thermal equilibrium. Third, the present results point out that, when examining the effect of membrane cholesterol on sPLA2, there is a need to use small cholesterol concentration increments over a wide concentration range. In most (if not all) previous studies on membrane cholesterol, large cholesterol concentration increments were used. In this case, a monotonic change in membrane properties with increasing cholesterol content was usually observed and the results were frequently attributed to the cholesterol-induced condensing effect on lipid acyl chains. In contrast to the conventional approaches, the present study used small cholesterol concentration increments (~0.3−1.0 mol %) over a wide range of cholesterol concentrations (e.g., 13−54 mol %). In this case, not only is the global cholesterol condensing effect revealed, but also the local biphasic activity change in the vicinity of critical cholesterol mole fractions is detected (Figure 1).

There are some data in support of the idea that cholesterol superlattice may occur in biological membranes. For example, in the normal human erythrocyte plasma membrane, cholesterol content relative to phospholipids is at ~40 mol %, which is one of the critical cholesterol mole fractions for the formation of centered rectangular superlattices (*20*). However, to find evidence for the existence of cholesterol superlattice in real biological membranes is a difficult task due to the complexity of the membrane. An alternative approach is to provide evidence for sterol superlattice formation in multicomponent lipid bilayers with integral membrane proteins at the density found in biological membranes. Although at present we have not yet accomplished this goal, we have obtained spectroscopic or semifunctional evidence for sterol regular distribution in dehydroergosterol/cholesterol/sphingomyelin/phosphatidylcholine (Wang, Brown, Sugar, and Chong, unpublished results) and in cholesterol/POPC/1-palmitoyl-2-oleoyl-L-α-phosphatidylethanolamine (*23*) multicomponent lipid bilayers. Thus, clearly, evidence for cholesterol superlattice formation is not limited to membranes comprised of one type of phospholipid. With regard to the limitation for cholesterol superlattice formation, we have found one, that is, the position of the double bonds in the fatty acyl chain of the matrix phospholipid (*50*). If the double bond is located between C2 and C9, then the spectroscopic evidence for sterol superlattice is abolished (*50*). However, phospholipids with double bonds between C2 and C9 are in small amounts in animal cell membranes except for nerve, sperm, and retinal membranes. Thus, the multicomponent studies suggested that cholesterol may still be regularly distributed in cholesterol/sphingomyelin/phosphatidylcholine-rich microdomains (separated from intrinsic membrane proteins) in some, but not all, biological membranes.

With this presumption in mind, we propose that the biphasic variation of oleic acid release from POPC at the critical cholesterol mole fractions (Figure 1C) might have important implications in the signaling pathways. POPC, the most abundant phosphatidylcholine in mammalian cells, contains a cis double bond between C-9 and C-10 in the *sn*-2 acyl chain (oleate), which is susceptible to sPLA2 hydrolysis. Long-chain *cis*-unsaturated fatty acids such as oleic acid are known to inhibit degranulation of cytotoxic T lymphocytes (CTL) (*51*) and the antigen-stimulated rise in CTL intracellular calcium levels (*52*) as well as CTL-mediated cytolysis (*53*). *Cis*-unsaturated fatty acids also inhibit tyrosine phosphorylation, a step essential for T cell activation (*54*). These inhibitory effects can be detected within seconds of fatty acid treatment, a time scale similar to that used in the determination of the initial hydrolytic rate of POPC by sPLA2 (Figure 1C). Furthermore, *cis*-unsaturated fatty acids stimulate protein kinase C activity (*55*, *56*). Thus, the alternating variation of the release rate of oleic acid with cholesterol (Figure 1C) implies that stimulation of protein kinase C and inhibition of degranulation of T cells may also be modulated by cholesterol content in an alternating manner in accordance with the principles of cholesterol regular distribution (*19*). In summary, the finding that the activity of sPLA2 is modulated up or down by minute changes in cholesterol content in the vicinity of a critical cholesterol mole fraction demonstrates a new type of regulation for sPLA2 activities and provides a new perspective for the functional importance of membrane cholesterol content.

REFERENCES

1. Dennis, E. A. (1994) *J. Biol. Chem. 269*, 13057−13060.
2. Wells, M. A. (1972) *Biochemistry 11*, 1030−1041.
3. Pieterson, W. A., Vidal, J. C., Volwerk, J. J., and De Haas, G. H. (1974) *Biochemistry 13*, 1455−1460.
4. Barlow, P. N., Lister, M. D., Sigler, P. B., and Dennis, E. A. (1988) *J. Biol. Chem. 263*, 12954−12958.
5. Gelb, M. H., Jain, M., and Berg, O. G. (1994) *FASEB J. 8*, 916−924.
6. Verger, R., Mieras, M. C. E., and de Haas, G. H. (1973) *J. Biol. Chem. 248*, 4023−4034.
7. Scott, D. L., White, S. P., Otwinowski, Z., Yuan, W., Gelb, M. H., and Sigler, P. B. (1990) *Science 250*, 1541−1546.

8. Op den Kamp, J. A. F., Kauer, M. T., and Van Deenen, L. L. M. (1975) *Biochim. Biophys. Acta 406*, 169−177.
9. Honger, T., Jorgensen, K., Biltonen, R. L., and Mouritsen, O. G. (1996) *Biochemistry 35*, 9003−9006.
10. Upreti, G. C., and Jain, M. K. (1980) *J. Membr. Biol. 55*, 113−121.
11. Huang, H.-W., Goldberg, E. M., and Zidovetzki, R. (1996) *Biochem. Biophys. Res. Commun. 220*, 834−838.
12. Menashe, M., Lichtenberg, D., Gutierrez-Merino, C., and Biltonen, R. L. (1981*) J. Biol. Chem. 256*, 4541−4543.
13. Menashe, M., Romero, G., Biltonen, R. L., and Lichtenberg, D. (1986) *J. Biol. Chem. 261*, 5328−5333.
14. Lichtenberg, D., Romero, G., Menashe, M., and Biltonen, R. L. (1986*) J. Biol. Chem. 261*, 5334−5340.
15. Burack, W. R., Yuan, Q., and Biltonen, R. L. (1993) *Biochemistry 32*, 583−589.
16. Chong, P. L.-G. (1996) in *High-Pressure Effects in Molecular Biophysics and Enzymology* (Markley, J. L., Northrop, D. B., and Royer, C. A., Eds.) pp 298−313, Oxford University Press, New York.
17. Chong, P. L.-G., Liu, F., Wang, M. M., Truong, K., Sugar, I. P., and Brown, R. E. (1996) *J. Fluoresc. 6*, 221−230.
18. Liu, F., Sugar, I. P., and Chong, P. L.-G. (1997) *Biophys. J. 72*, 2243−2254.
19. Chong, P. L.-G. (1994) *Proc. Natl. Acad. Sci. U.S.A. 91*, 10069−10073.
20. Virtanen, J. A., Ruonala, M., Vauhkonen, M., and Somerharju, P. (1995) *Biochemistry 34*, 11568−11581.
21. Sugar, I. P., Tang, D., and Chong, P. L.-G. (1994) *J. Phys. Chem. 98*, 7201−7210.
22. Chong, P. L.-G., Tang, D., and Sugar, I. P. (1994) *Biophys. J. 66*, 2029−2038.
23. Wang, M. M., Sugar, I. P., and Chong, P. L.-G. (1998) *Biochemistry 37*, 11797−11805.
24. Bartlett, G. R. (1959) *J. Biol. Chem. 234*, 466−468.
25. Richieri, G. V., Ogata, R. T., and Kleinfeld, A. M. (1992) *J. Biol. Chem. 267*, 23495−23501.
26. Lowry, O. H., Rosebrough, N. J., Farr, A. L., and Randall, R. J. (1951) *J. Biol. Chem. 193*, 265−275.
27. Hope, M. J., Bally, M. B., Webb, G., and Cullis, P. R. (1985*) Biochim. Biophys. Acta 812*, 55−65.
28. Ghoshroy, K. B., Zhu, W., and Sampson, N. S. (1997) *Biochemistry 36*, 6133−6140.
29. Richieri, G. V., and Kleinfeld, A. M. (1995) *Anal. Biochem. 229*, 256−263.
30. She, H. S., Garsetti, D. E., Steiner, M. R., Egan, R. W., and Clark, M. A. (1994) *Biochem. J. 298*, 23−29.
31. Somerharju, P. J., Virtanen, J. A., Eklund, K. K., Vainio, P., and Kinnunen, P. K. J. (1985) *Biochemistry 24*, 2773−2781.
32. Tang, D., and Chong, P. L.-G. (1992) *Biophys. J. 63*, 903−910.
33. Cheng, K. H., Ruonala, M., Virtanen, J., and Somerharju, P. (1997) *Biophys. J. 73*, 1967−1976.
34. Virtanen, J. A., Cheng, K. H., and Somerharju, P. (1998) *Proc. Natl. Acad. Sci. U.S.A. 95*, 4964−4969.
35. Henshaw, J. B., Olsen, C. A., Farnbach, A. R., Nielson, K. H., and Bell, J. D. (1998) *Biochemistry 37*, 10709−10721.
36. Kupferberg, J. P., Yokoyama, S., and Kezdy, F. J. (1981) *J. Biol. Chem. 256*, 6274−6281.
37. Apitz-Castro, R., Jain, M. K., and De Hass, G. H. (1982) *Biochim. Biophys. Acta 688*, 349−356.
38. Bell, J. D., and Biltonen, R. L. (1992) *J. Biol. Chem. 267*, 11046−11056.
39. Wood, R., and Lee, T. (1983) *J. Chromatogr. 254*, 237−246.
40. Demel, R. R., Geurts van Kessel, W. S. M., and Van Deenen, L. L. M. (1980) *Biochim. Biophys. Acta 266*, 26−40.
41. Huang, C., and Mason, J. T. (1982) in *Membrane and Transport* (Martosoni, A. N., Ed.) Vol. 1, pp 15−23, Plenum Publishing, New York.
42. Okimasu, E., Sasaki, J., and Utsumi, K. (1984) *FEBS Lett. 168*, 43−48.
43. Parasassi, T., Giusti, A. M., Raimondi, M., and Gratton, E. (1995) *Biophys. J. 68*, 1895−1902.
44. Huang, J., Buboltz, J., and Feigenson, G. W. (1998) *Biophys. J. 74*, A314.
45. Virtanen, J. A., Somerharju, P., and Kinnunen, P. K. J. (1988) *J. Mol. Electron. 4*, 233−236.
46. Needham, D., and Nunn, R. S. (1990) *Biophys. J. 58*, 997−1009.
47. Fraenkel-Conrat, H., Jeng, T. W., and Hsiang, M. (1980) in *Natural Toxins* (Eaker, D., and Wadstrom, T. E., Eds.) pp 561−567, Pergamon, Oxford, U.K.
48. Faure, G., and Bon, C. (1988) *Biochemistry 27*, 730−738.
49. Lichtenbergova, L., Yoon, E. T., and Cho, W. (1998) *Biochemistry 37*, 14128−14136.
50. Wang, M. M., and Chong, P. L.-G. (1999) *Biophys. J. 76*, A59.
51. Anel, A., Richieri, G. V., and Kleinfeld, A. M. (1994) *J. Biol. Chem. 269*, 9506−9513.
52. Richieri, G. V., and Kleinfeld, A. M. (1989) *J. Immunol. 143*, 2302−2310.
53. Richieri, G. V., and Kleinfeld, A. M. (1990) *J. Immunol. 145*, 1074−1077.
54. O'Rourke, A. M., and Mescher, M. F. (1992) *Nature 358*, 253−255.
55. Shinomura, T., Asaoka, Y., Oka, M., Yoshida, K., and Nishizuka, Y. (1991*) Proc. Natl. Acad. Sci. U.S.A. 88*, 5149−5153.
56. Khan, W. A., Blobe, G. C., and Hannun, Y. A. (1992) *J. Biol. Chem. 267*, 3605−3612.

BI982693Q